

1 *Supplement of*

2 **Suppressed atmospheric chemical aging of cooking organic aerosol**  
3 **particles in wintertime conditions** by

4 Wenli Liu et al.

5

6 *Correspondence to: Kuwata Mikinori (kuwata@pku.edu.cn)*

7

8

## 9 Text S1. ME-2 analysis

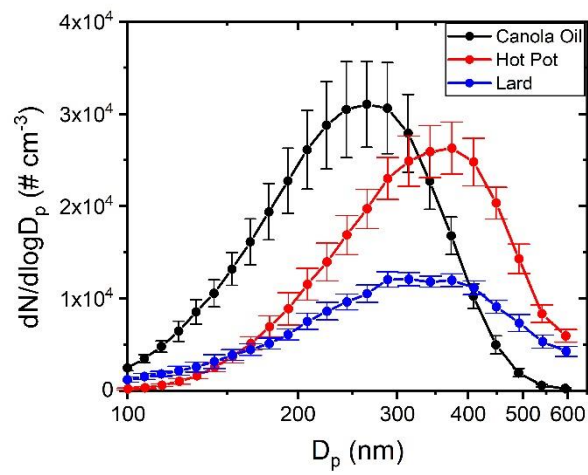
10 ME-2 analysis was used to estimate mass fractions of ‘fresh COA’ and ‘oxidized COA’ in  
11 particles for each experimental condition. 10~15 sets of mass spectra with the range of  $m/z =$   
12 41 to 210, excluding 44, at each position were employed for the analysis. The mass spectra of  
13 COA particles prior to ozone exposure were employed as seed profiles for the analysis. The  
14 mass spectra for the high ozone exposure (7 ppm, 60 s of exposure time) at 25 °C were analyzed  
15 together with each experimental dataset to constrain the profiles for reaction products.

16 The number of factors was changed for the range of 2 to 4 to evaluate the appropriate  
17 factor number using the data for Exp. #1. The resulting ratio of the sum of squared residuals  
18 weighted ( $Q$ ) by their uncertainties to the degree of freedom of model solution calculated based  
19 on the size of the data matrix and the number of factors ( $Q_{exp}$ ) is one important metric to judge  
20 the appropriateness of the solution.  $Q/Q_{exp}$  values decreased from 1.9 to 1.47 as factor numbers  
21 increased from 2 to 3. For the 4-factor analysis, it kept decreasing but was not that significant  
22 (1.29).

23 In the case of 2-factor analysis, dominated ions in the mass spectra (Fig. S4) were almost  
24 the same for the two factors. However, the factor analysis successfully resolved marker ions for  
25 ‘fresh COA’ (e.g.,  $m/z = 191$  and  $202$ ) and certain reaction products (e.g.,  $m/z = 155$ ). Mass  
26 spectra for the factors in the 3-factor analysis are shown in Fig. S12. Factor 1 exhibited a very  
27 high correlation ( $R^2 > 0.999$ ) with the seed profile, which was treated as the ‘fresh COA’. Peak  
28 at  $m/z = 155$ , the marker ion for ‘oxidized COA’, was significant in factor 2. Changes in mass  
29 fraction at each data point (Fig. S13) reconfirmed that factor 1 and factor 2 corresponded to  
30 ‘fresh COA’ and ‘oxidized COA’. The mass spectrum of factor 3 showed higher similarity with  
31 factor 2. The contribution of factor 3 was negligible except for the high ozone exposure period.  
32 We speculate that the factor might correspond to reaction products that are not produced by the  
33 initial ozonolysis. The existence of factor 3 does not influence the estimation of  $k_2$ , as we  
34 employed the loss of ‘fresh COA’ for calculating the parameter. No factor in the 4-factor  
35 analysis corresponded to the ‘fresh COA’ (Fig. S14). As a result, two-factor solutions were  
36 employed in the present research. (Budisulistiorini et al., 2021; Liu et al., 2023)

37 The degree of freedom ( $a$ -value) was also changed from 0.0 to 1.0 with the interval of 0.1  
38 for optimizing the analysis. Figure S15 shows the corresponding  $Q/Q_{exp}$  values for Exp. #1, 7,  
39 9, 10, 20 and 21. The  $Q/Q_{exp}$  values decreased significantly when the  $a$ -value increased from 0  
40 to 0.1. The value slightly decreased from 0.1 to 0.2. No apparent change in the  $Q/Q_{exp}$  values  
41 was observed for higher  $a$ -values. The mass spectra of factor 1 for the above-mentioned  
42 experimental runs exhibited a high correlation ( $R^2 > 0.999$ ) with the seed profile among all the  
43  $a$ -value tests. We set the  $a$ -value to be 0.2 in the present study, based on the above-mentioned  
44 conditions.

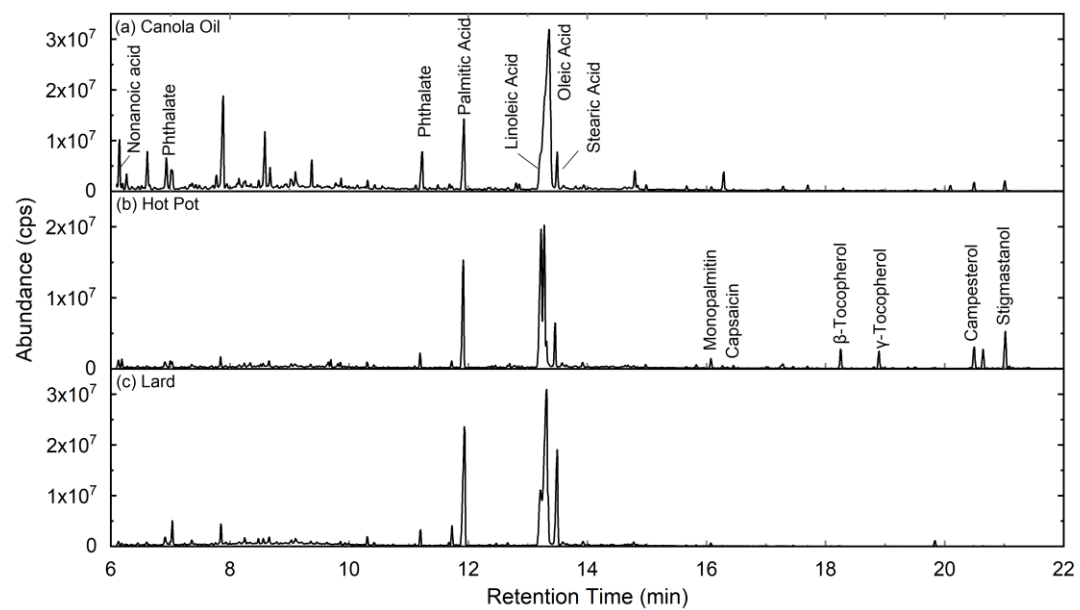
45



46

47 **Figure S1.** Size distributions of laboratory generated COA particles following coagulation. Size  
 48 distributions of particles were recorded every 3 minutes in 60 bins for the diameter range of 10  
 49 and 600 nm (only the range of 100 to 600 nm is shown).

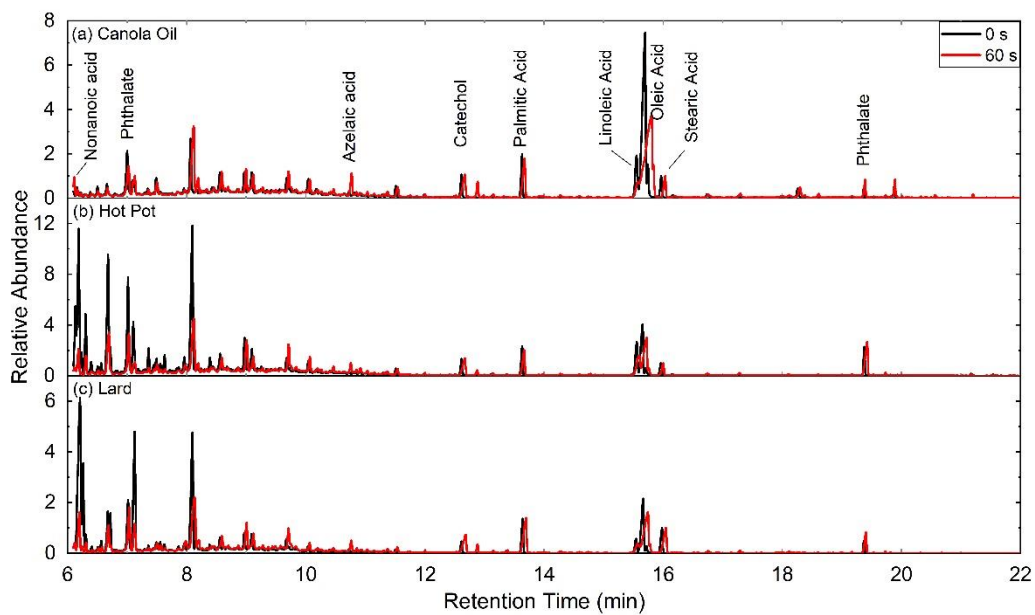
50



51

52 **Figure S2.** Gas chromatograms of (a) canola oil; (b) hot pot and (c) lard COA particles.

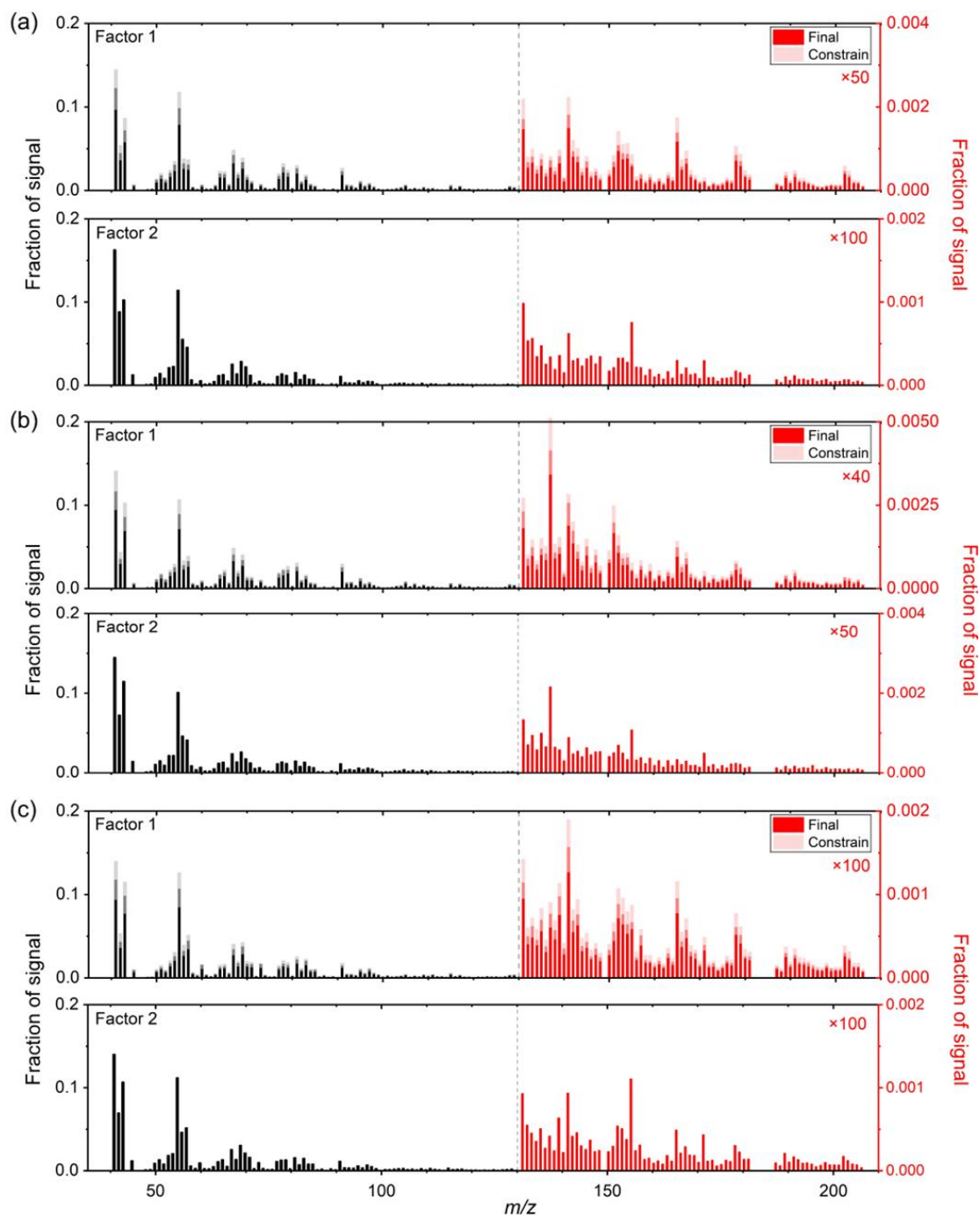
53



54

55 **Figure S3.** Gas chromatograms of (a) canola oil; (b) hot pot and (c) lard COA particles for prior  
 56 (black) and following  $2.7 \times 10^{-5}$  atm s of ozone exposure (red). The abundances are normalized  
 57 by the intensity of stearic for each measurement.

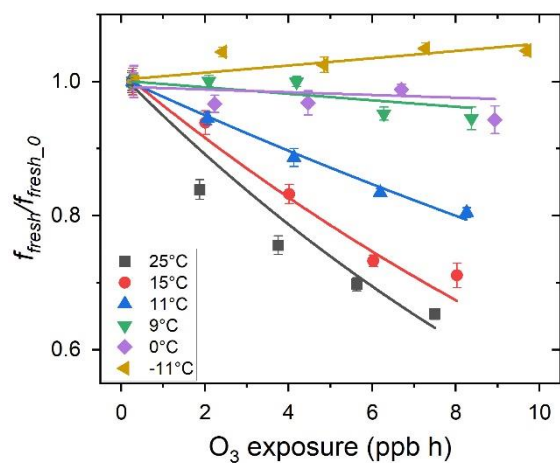
58



59

60 **Figure S4.** Mass spectra of factor 1 and factor 2 for (a) canola oil Exp. #1; (b) hot pot Exp. #9;  
 61 (c) lard Exp. #20 COA particles. Dark color bars indicate the resulting profile from the factor  
 62 analysis, while the light color bars correspond to the constrained ranges for factor 1 during the  
 63 analysis. The signal fractions of  $m/z$  of 130~210 are enhanced by different times as noted on  
 64 the graph.

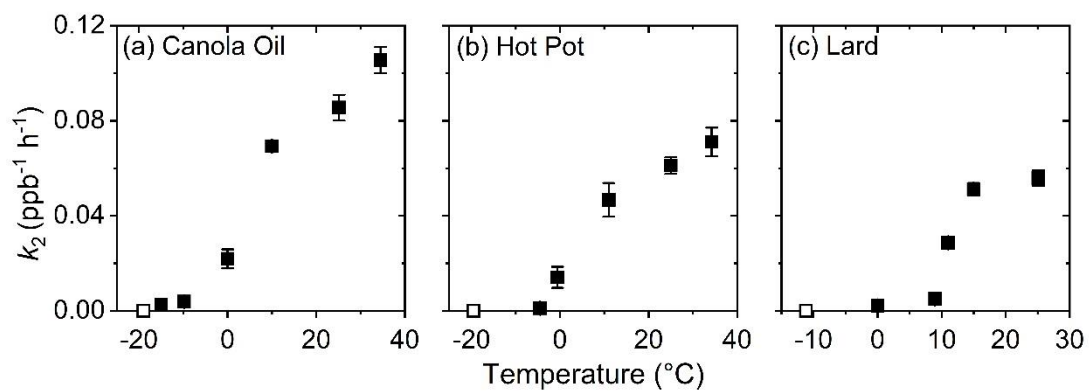
65



66

67 **Figure S5.** Changes in mass fractions of ‘fresh COA’ ( $f_{fresh}$ ) for lard experiments induced by  
 68 ozone exposure. The value of  $f_{fresh}$  prior to ozone exposure was denoted as  $f_{fresh-0}$ . The data were  
 69 colored by temperature of the flow tube. The positive slope for fitting line for -11°C experiment  
 70 was not employed for the calculation of  $k_2$ .

71

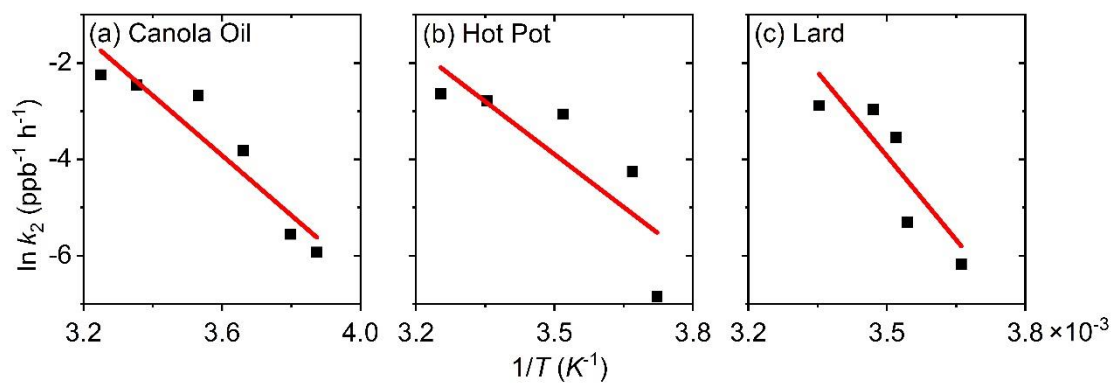


72

73 **Figure S6.** Values of  $k_2$  for (a) canola oil, (b) hot pot, and (c) lard COA particles at various  
 74 temperatures. The values of  $k_2$  for Exp. #7, 10 and 21 were unmeasurably small for our  
 75 experimental setup. Thus, they were shown in open symbols at the bottom.

76

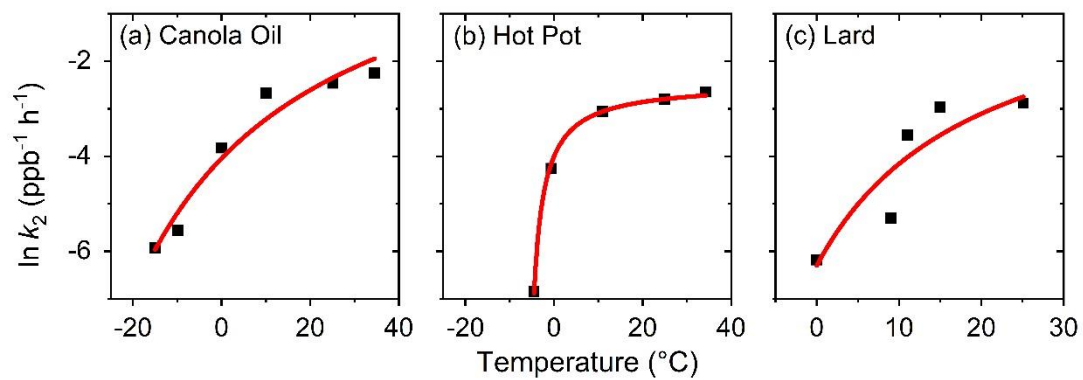




77

78 **Figure S7.**  $k_2$ - $T$  relationship of (a) canola oil, (b) hot pot, and (c) lard COA particles fit by the  
 79 Arrhenius equation  $\ln k_2 = \ln A - \frac{E_a}{RT}$ .

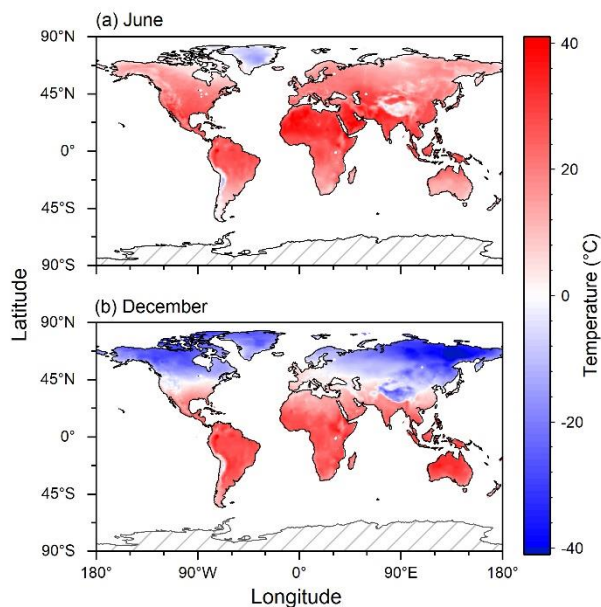
80



81

82 **Figure S8.**  $k_2$ - $T$  relationship of (a) canola oil, (b) hot pot, and (c) lard COA particles fit by the  
 83 Vogel–Fulcher–Tammann (VFT) equation  $\ln k_2 = \alpha_1 + \frac{\alpha_2}{T+\alpha_3}$ .

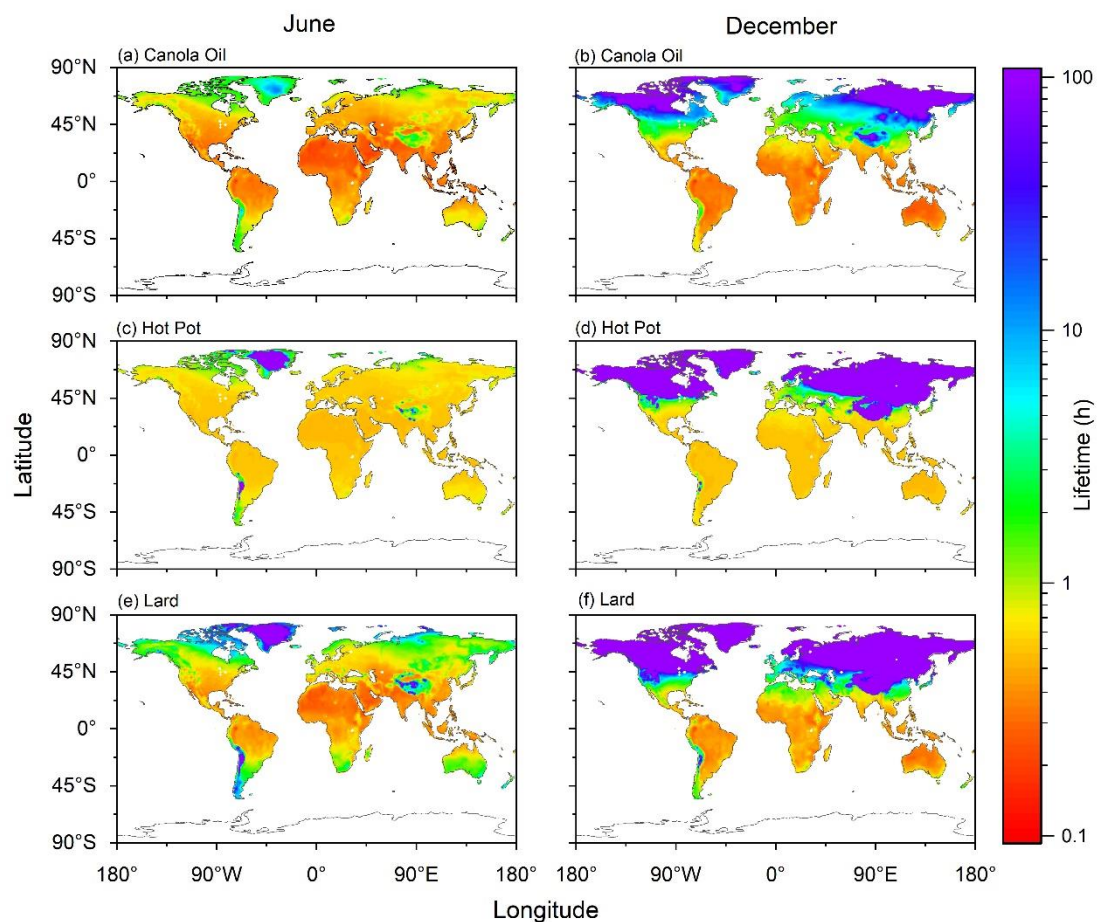
84



85

86 **Figure S9.** Monthly mean surface air temperatures during (a) June and (b) December of 2021.  
87 Data were obtained from the website of the Physical Sciences Laboratory of NOAA  
88 (<https://psl.noaa.gov/mddb2/makePlot.html?variableID=1603>).

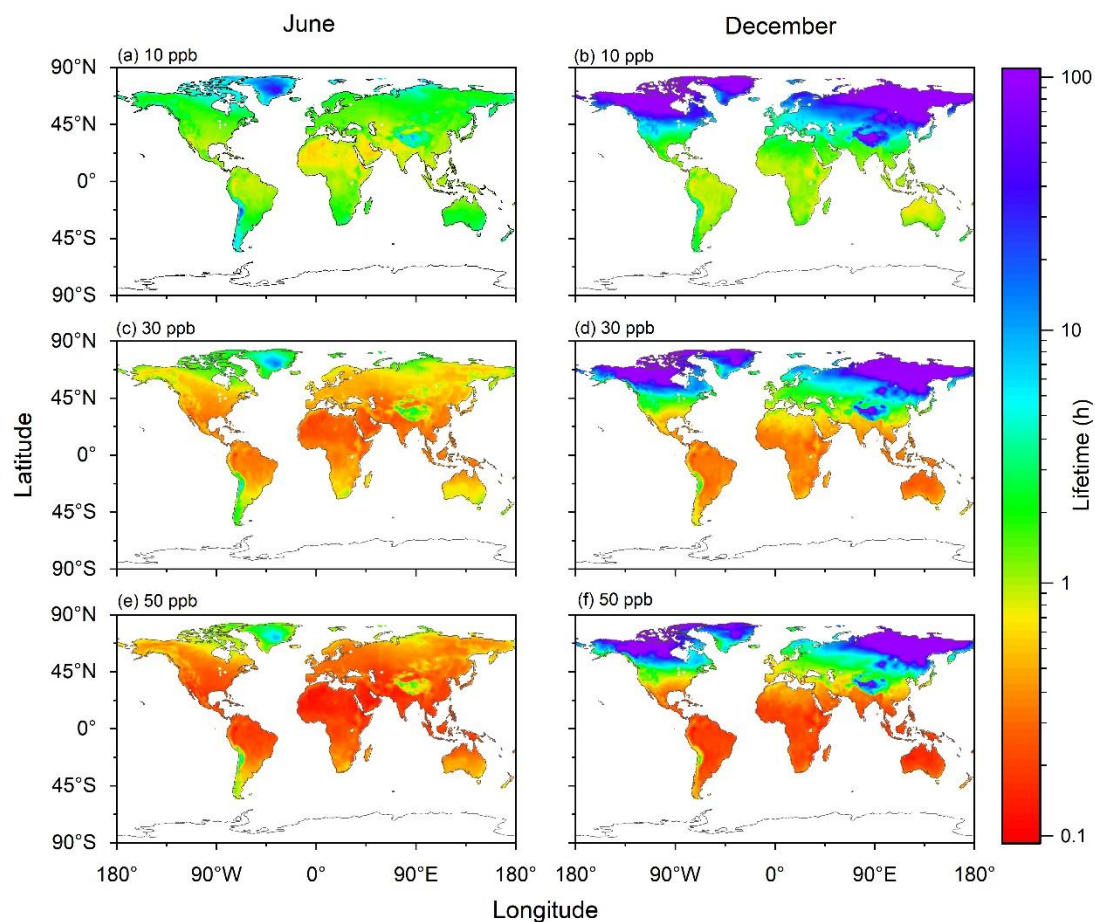
89



90

91 **Figure S10.** The estimated atmospheric chemical lifetime of cooking organic aerosols during  
 92 (a,c,e) June and (b,d,f) December. Relationships between reaction rate constants  $k_2$  and  
 93 temperature were from the parameterization of (a,b) canola oil; (c,d) pot hot and (e,f) lard  
 94 experiment results. Ozone concentration was assumed as 30 ppb.

95

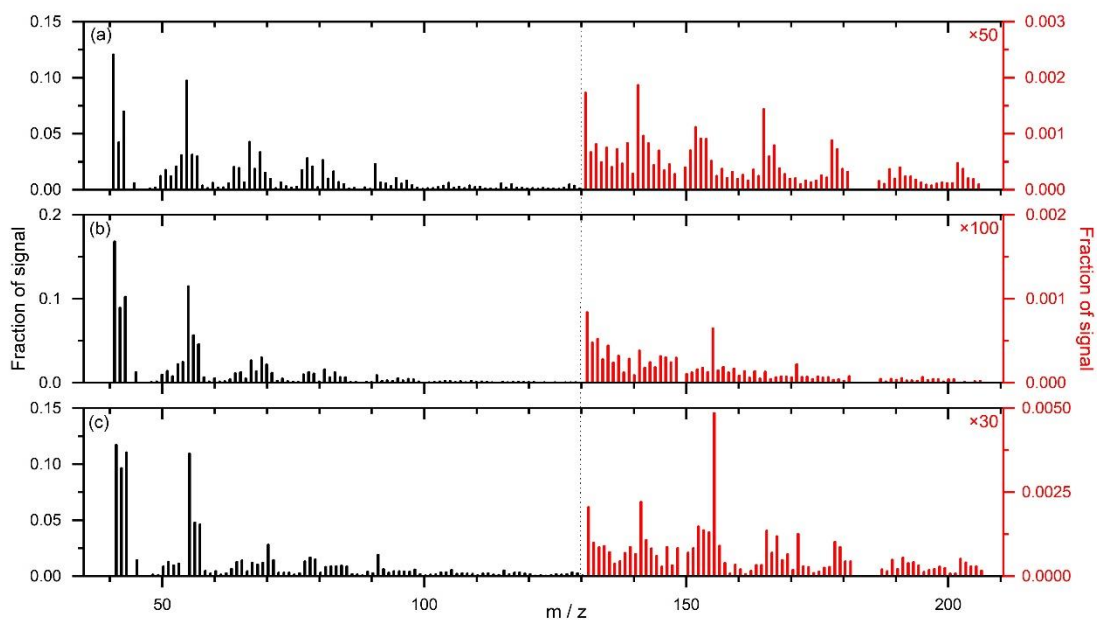


96

97 **Figure S11.** The estimated atmospheric chemical lifetime of cooking organic aerosols during  
 98 (a,c,e) June and (b,d,f) December. The  $k_2$ - $T$  relationship for the canola oil experiment results  
 99 were employed. Ozone concentrations were assumed to be (a,b) 10 ppb; (c,d) 30 ppb and (e,f)  
 100 50 ppb.

101

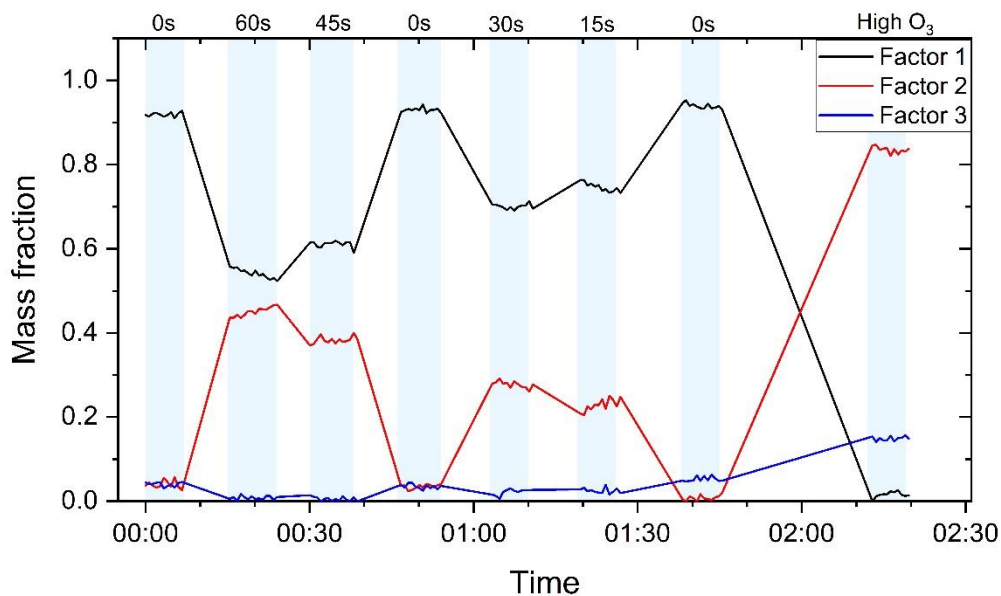
102



103

104 **Figure S12.** Mass spectra of (a) factor 1, (b) factor 2 and (c) factor 3 for the 3-factor analysis  
105 for canola oil Exp. #1. The signal fractions of  $m/z$  of 130~210 are enhanced by different times  
106 as noted on the graph.

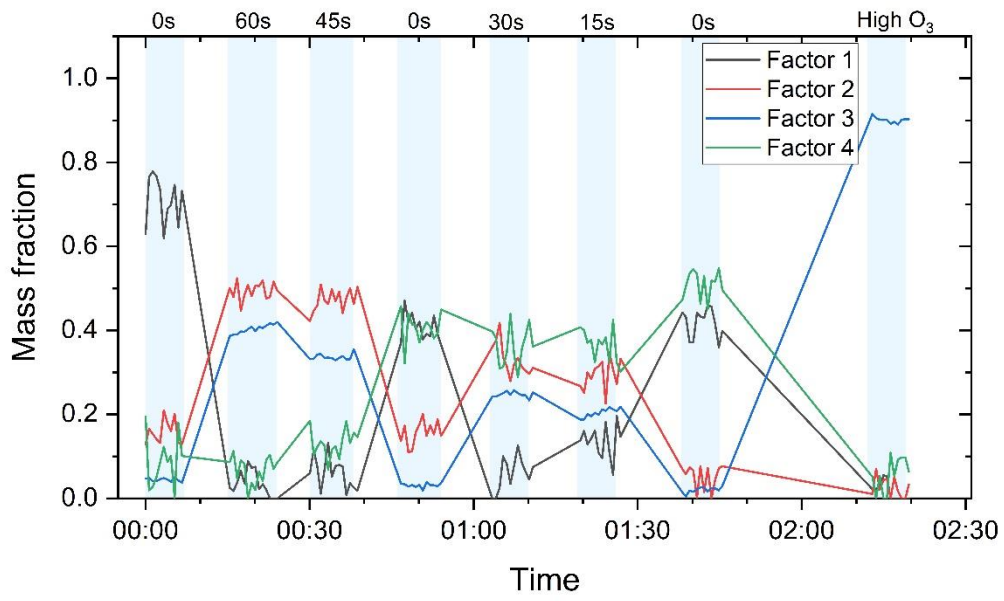
107



108

109 **Figure S13.** Time series plot for the contributions of three factors in the 3-factor analysis of  
 110 canola oil Exp. #1. Values at the top indicate the reaction time for COA particles with ozone.  
 111 Ozone concentration was 7 ppm for the 'High O<sub>3</sub>' period.

112

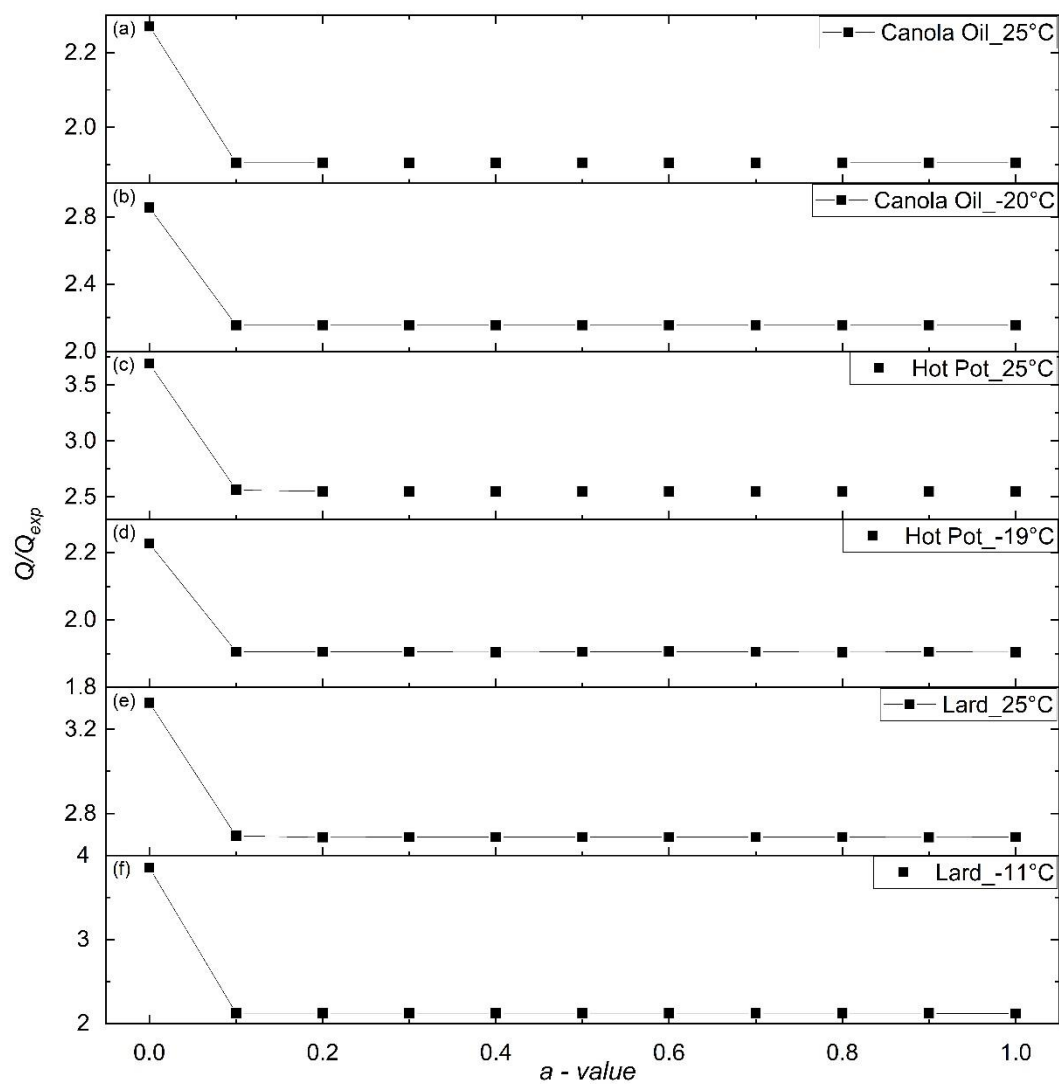


113

114 **Figure S14.** Time series plot for the contributions of the four factors in the 4-factor analysis of  
 115 canola oil Exp. #1.

116





117

118 **Figure S15.** Dependence of  $Q/Q_{exp}$  values on  $a$ -value for the ME-2 analyses of (a, b) canola oil  
 119 (c, d) hot pot and (e, f) lard experiments at room and the lowest temperatures.

120

121 **Table S1.** Summary of the experiments for the present study.

Exp. #	Particles	$T$ (°C)	Analysis
1	Canola Oil	25	ACSM and SEMS
2	Canola Oil	-15	ACSM and SEMS
3	Canola Oil	10	ACSM and SEMS
4	Canola Oil	0	ACSM and SEMS
5	Canola Oil	-10	ACSM and SEMS
6	Canola Oil	34.5	ACSM and SEMS
7	Canola Oil	-19	ACSM and SEMS
8	Canola Oil	25	SV-TAG and OPC
9	Hot Pot	25	ACSM and SEMS
10	Hot Pot	-19.5	ACSM and SEMS
11	Hot Pot	-4.5	ACSM and SEMS
12	Hot Pot	-0.5	ACSM and SEMS
13	Hot Pot	34	ACSM and SEMS
14	Hot Pot	11	ACSM and SEMS
15	Hot Pot	25	SV-TAG and OPC
16	Lard	0	ACSM and SEMS
17	Lard	15	ACSM and SEMS
18	Lard	9	ACSM and SEMS
19	Lard	11	ACSM and SEMS
20	Lard	25	ACSM and SEMS
21	Lard	-11	ACSM and SEMS
22	Lard	25	SV-TAG and OPC

122

123 **Table S2.** Standards used for SV-TAG in the present study.

Calibration standards in experiment		
Compound	Purity	Company
Oleic acid	99.8%	Shanghai Macklin Biochemical Co., Ltd
Linoleic acid	99%	Shanghai Macklin Biochemical Co., Ltd
Stearic acid	99%	Shanghai Aladdin Biochemical Technology Co., Ltd
Palmitic acid	99%	Shanghai Aladdin Biochemical Technology Co., Ltd

124

125

126 **Table S3.** Optimized parameters of Vogel–Fulcher–Tammann (VFT) equation fitting for three  
127 COA.

	$\alpha_1$	$\alpha_2$	$\alpha_3$
Canola Oil	1.67	-340.6	59.6
Hot Pot	-2.46	-10.6	6.9
Lard	0	-111.4	17.9

128

129 **Reference**

130

131 Budisulistiorini, S. H., Chen, J., Itoh, M., and Kuwata, M.: Can online aerosol mass  
132 spectrometry analysis classify secondary organic aerosol (SOA) and oxidized primary  
133 organic aerosol (OPOA)? A case study of laboratory and field studies of Indonesian  
134 biomass burning, ACS Earth Space Chem., 5, 3511-3522,  
135 <https://doi.org/10.1021/acsearthspacechem.1c00319>, 2021.

136 Liu, W., Liao, K., Chen, Q., He, L., Liu, Y., and Kuwata, M.: Existence of crystalline  
137 ammonium sulfate nuclei affects chemical reactivity of oleic acid particles through  
138 heterogeneous nucleation, J. Geophys. Res.: Atmos., 128, e2023JD038675,  
139 <https://doi.org/10.1029/2023JD038675>, 2023.

140